# MODELING A SRM BASED FLYWHEEL ENERGY STORAGE SYSTEM

Antonio Carlos Ferreira[1], José Luiz Da Silva Neto[2], Luis Guilherme Barbosa Rolim[1,2], Rubens De Andrade Junior[2]

[1]Prog. Eng. Elétrica/COPPE/UFRJ [2] Depto Eng. Elétrica/Escola Politécnica/UFRJ
ferreira@ufrj.br, luineto@dee.ufrj.br, rolim@dee.ufrj.br, randrade@dee.ufrj.br

*Abstract* – **The aim of this paper is to present a dynamic model of a SRM motor-generator which takes magnetic non-linearity into account, applied to a flywheel energy storage system. The developed model differs from previous models found in the literature for it explores the real non-linear characteristics of the machine, i.e. the dependency of the inductance and torque on both rotor position and stator current. The key aspect of the presented model is that it can be implemented in most power system and power electronics simulators, allowing the simulation of the complete system model. The control and power circuitries are also described. Finally simulations are presented which illustrate the system operation.**

*Keywords* – **Flywheel, Power quality, Switched reluctance machine.**

## I. INTRODUCTION

IN modern production plants, voltage sags can cause slow output, production interruption or damage to machines. Energy customers with continuous processes involving fragile materials, like paper forming, food processing, etc, are likely to suffer economic losses with interruptions due the energy quality problems like voltage sags. Dynamic voltage restorers (DVRs) can compensate voltage sags avoiding these losses, but some of these devices draw the energy necessary to compensate the voltage sags from the same grid that they will compensate. This strategy can cause a system failure in some cases. In order to avoid this failure, these equipments may employ energy storage devices as electrochemical batteries and flywheel energy storage systems [1]. ]. The flywheels are more robust and reliable than the electrochemical batteries and can replace it if their energy density will be increased.

The energy stored in a flywheel is proportional to the moment of inertia and the square of angular velocity. Then increasing the flywheel angular velocity may increase the energy density of FESS [2]. But in high speed rotating devices the dynamic mechanical stability plays an important role. The critical speeds of the whole structure have to be known and avoided in the regular operation. The critical speeds are that ones where natural mechanical vibration modes can be excited. In order to conduct mechanical simulations to predict the critical speeds of the whole system, the dynamic characteristics of the bearings and motor-generator have to be known. Also the torque ripple can excite the natural vibrations modes. The electrical dynamical model for the SRM motor-generator is important not only for the simulation of the electromechanical energy conversion between the flywheel and the electrical system, but also for the mechanical designing of the whole system.Other significant aspect of the energy storage device is concerned to the electromechanical energy conversion between the flywheel and the electrical system. The aim of this paper is to present a dynamic model of the SRM motor-generator which takes magnetic non-linearity into account, applied to a flywheel energy storage system. The developed model differs from previous models found in the literature [3] for it explores the real non-linear characteristics of the machine, i.e. the dependency of the inductance and torque on both rotor position and stator current. The key aspect of the presented model is that it can be implemented in most power system and power electronic simulators, allowing the simulation of the complete system model. The control and power circuitries are also described. Finally simulations are presented which illustrate the system operation.

## II. SWITCHED RELUCTANCE MACHINE MODEL

The operation of a switched reluctance machine (SRM) is based on the principle of minimal reluctance and continuous movement of the rotor is achieved exciting the stator phases sequentially [4]. Symmetry of the magnetic circuit normally allows for nearly null mutual flux linkage, even under saturated condition. As a result, the contribution of each phase for torque production is mainly defined by the self-inductance profile of that phase. The electromagnetic torque can be generally obtained from the co-energy as shown by equation (1), where $T_e$ is the electromagnetic torque, $\theta_r$ is the rotor angular position, W' is the co-energy and *i* is the coil current. The electromagnetic torque produced by one single coil is then given by equation (2), where $\lambda$ is the total flux linked to the coil.

$$T_e(i) = \left( \frac{\partial W'(\theta_r)}{\partial \theta_r} \right)_{i=cte} \tag{1}$$

$$T_e(\theta_r, i_L) = \frac{\partial}{\partial \theta_r} \left[ \int_0^i \lambda(\theta_r, i_L) di \right] \tag{2}$$

Both relationships $T_e(\theta_r, i)$ and $\lambda(\theta_r, i)$ are strongly non-linear, a fact that makes it difficult to develop an analytical mathematical model for the SRM. Thus instead of trying to obtain such an analytical model, the methodology adopted in this work was to use tabulated data for $T_e(\theta_r, i)$ and $\lambda(\theta_r, i)$, which may have been obtained off-line by means of static measurements or FEM computations. The tabulated data is then used, with linear interpolation, directly in the solution of the electrical and mechanical dynamic equations (3) and (4), where V is the coil terminal voltage, $r_s$ is the coil resistance and $i$ is the current flowing through the coil.

$$V = r_s \cdot i_L + \frac{d\lambda(\theta_r, i_L)}{dt} \tag{3}$$

$$J \cdot \frac{d^2\theta_r}{dt^2} = T_{eT} - T_m \tag{4}$$

In equation (4), J is the combined moment of inertia (SRM rotor plus flywheel), $T_e$ is the electromagnetic torque and $T_m$ is the load opposing torque and mechanical losses. Figs. 1 and 2 show the tabulated data obtained from finite-elements simulations of a 6/4 SRM, which model is verified in this work.

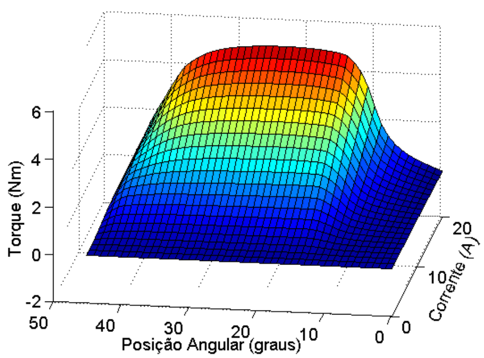


Fig 1. Electromagnetic torque obtained from finite-elements simulation.

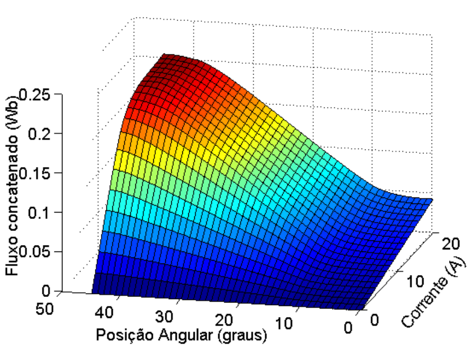


Fig. 2. Flux linkage obtained from finite-elements simulation.

Unfortunately equation (3) cannot be properly digitally solved in this form. In order to simulate the electrical phase equations of the SRM, they must be put in an appropriate form, suitable to be applied in most circuit simulation software. The second term on the right side of (3) represents a voltage drop on a non-linear multi-variable dependent inductance, which is not available as a fundamental circuit element in most circuit simulation software.

Modeling inductive non-linear relations involving rotating magnetic circuits is not straightforward. Accordingly, several different methodologies to model SRM's magnetic behavior are reported in the literature [7][8][9][10]. The approach used in this work is based on the v-i relationship in an inductor, given by equations (5) and (6).

$$v_L(t) = L\frac{di_L(t)}{dt} \tag{5}$$

$$i_L(t) = \frac{1}{L}\int v_L(t)dt + i_L(0) \tag{6}$$

Equation (6) is obtained by solving (5) for $i_L(t)$ and suggests that an inductance can be modeled as a controlled current source. The electrical torque $T_e(\theta_r, i_L)$ can also be obtained from tabulated data. Fig. 3 illustrates the implementation for the SRM of the per-phase model of the inductance developed in this work, where the tabulated data representing the non-linear magnetic characteristics is incorporated in a *look-up table type* block.

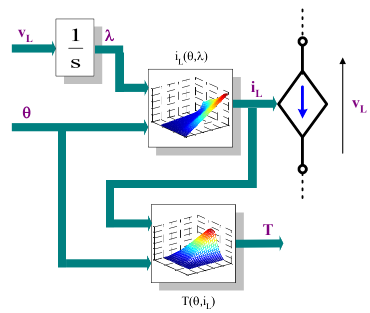


Fig. 3. Model of one phase inductance of the SRM

## III. POWER AND CONTROL CIRCUITS

In this work an asymmetrical bridge is used as the power circuit responsible for the current control. The main feature of this topology is the two-quadrant operation, allowing for reversibility of the applied voltage with unidirectional current which is crucial for fast current extinction in motoring operation, and for the correct current control in the regenerating mode. For the current synthesis the strategy adopted is the PWM control with hysteresis band. According to the required energy flow direction, the switching sequence determines three different states (Fig. 4) for the power circuit.

In STATE 1 the energy flows from the DC link to the machine. In STATE 2 the current falls freely if the angular interval of conduction determines a positive torque for positive angular speed. Otherwise, for positive speed and negative torque, the phase current will tend to increase due to the negative sign of the factor $\frac{\partial\lambda}{\partial\theta}\frac{d\theta}{dt}$. This term can be viewed as a "speed voltage" obtained from the expansion of $\frac{d\lambda(\theta_r, i_L)}{dt}$.

Finally, in STATE 3 the converter injects current into the DC link regenerating energy. In all three states the current flows through the stator phase in the same direction. In spite of the converter's two-quadrant operation capability, the SRM can be continuously operated in any quadrant of the torque-speed plane. However, for regenerating action to occur [5][6], it is mandatory that STATE 3 is used for longer times than the other states during any current pulse.

The use of STATE 1 and STATE 2 for phase current pulse shaping is known as unipolar or "soft" chopping, which is commonly used in motoring operation. Bipolar or "hard" chopping uses STATE 2 and STATE 3 [4]. It can also be used for motoring, but switching losses will be higher in that case. Yet during regeneration, current control can only be achieved if bipolar chopping is used.

Fig. 5 exemplifies occurrence of all the three states of the power converter during a phase current pulse with hysteresis PWM current control. Two cases are shown: a) positive speed and positive torque (motoring); b) positive speed and negative torque (regenerating).

Since each state ultimately define the voltage applied to the stator phases, the behavior of the power converter can be modeled by switching functions. This approach is particularly interesting to be employed in some simulation software having convergence problems or inherently slow execution rate, like MATLAB/SIMULINK. Modeling static switches involves determining the zero-crossing instants, which can be very time-consuming, depending on the algorithm for solving non-linear differential equations. Therefore, it is possible to model the converter using voltage sources controlled by switching functions. For the SRM drive one can define the function *p* that can assume values 1, 0 or –1 according to states 1, 2 and 3 respectively. The voltage $V_L$ applied to one stator phase is then calculated by (7), where $V_F$ and $V_{CEsat}$ are the voltages across the diodes and transistors respectively. The *dc* link total current is simply calculated by (8), where $I_{L1}$, $I_{L2}$ and $I_{L3}$ are the stator phases currents.

$$V_L = pV_{dc} + (p-1)V_F - (1+p)\,V_{CEsat} \quad (7)$$

$$I_{dc} = p_1 I_{L1} + p_2 I_{L2} + p_3 I_{L3} \quad (8)$$

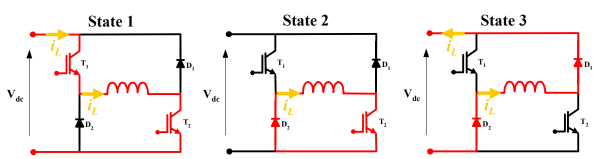


Fig. 4 Operating states of the power circuit

## IV. MODEL VALIDATION

In order to verify the SRM drive model by simulation, initially a simple speed control was considered, exploring operation with positive and negative torque. A **PI** (*Proportional + Integral*) controller was used, producing the reference current for the active phases PWM current controllers.

The logic for determining the operation as motor or generator and the PWM control for a 6/4 SRM is presented by the abstract code in Fig. 6. Each stator phase conducts for approximately 30 mechanical degrees on either motoring or regenerating modes. In Fig. 6: $\theta_{ON}$, $\theta_{OFF}$ are the angles for, respectively, the triggering and blocking the current circulation; $\mathbf{i_L}$ , $\mathbf{i_L^{ref}}$ are respectively the measured and the reference current; $\mathbf{\Delta i}$ is the hysteresis current band; and $\omega$ is the angular speed.

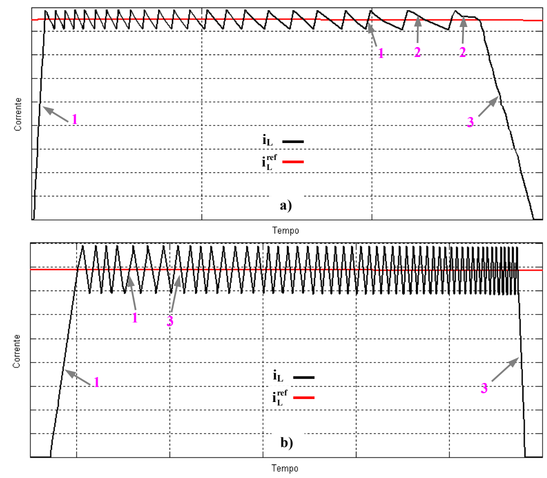


Fig. 5 PWM control with hysteresis band: unipolar (a) and bipolar (b) switching.

The SRM drive was modeled in the PSCAD/EMTDC based on a real 1.5 kW prototype. Fig. 7 shows the simulation results where the **PI** parameters were chosen to impose an under-dumped dynamics in order to illustrate the two modes of operation. One can see that a positive current reference determines a motor operation mode, while a negative reference indicates the operation in the regenerating mode.

In order to validate the model, tests were carried out in a test rig. The main components are: 1.5 kW 6/4 SRM, bidirectional converter with a dc link capacitor and a Superconductor Magnetic Thrust Bearing, which would also work as a flywheel increasing the system inertia. The coupling between the SRM rotor shaft and the bearing is assumed to be rigid so they were represented as a single inertia. The agreement between measurements and simulated results can be better illustrated in Fig. 8, which shows the current in one stator phase when the system is operating in the single pulse mode. The machine was running in open-loop at 1000 rpm with 9 V in the dc link, opposing to the normal closed-loop operating voltage (>400V). The parameters used in the SRM model were obtained from Finite Element simulations. The small differences observed in Fig. 8 are due, mainly, to the low dc voltage. Normally the forward voltage drop in the power electronic devices is not significant when compared to the dc link voltage, and then do not need to be precisely modeled.

In order to demonstrate the flywheel operation with the developed PSCAD/EMTDC model, a simulation was carried out where, for simplicity but without loss of generality, the connection to the power grid was modeled by a current source connected directly to the dc link. The intention was to study the performance of the control loop when energy is injected or drawn from the link. Fig. 9 shows the simplified circuit. The simulation results are shown in Fig. 10. At t=0s a 10A current is solicited from the *dc* link by the grid, imposing that the SRM operates as a generator. The situation is reversed at t=6s when the grid injects energy into the capacitor, which voltage remained regulated, at small rate in order to restore the reference speed.

```
if (iL^ref ≠ 0)
 {
   if (ω = 0)
    {
      if (iL^ref < 0)
       {
         θON ↔ θOFF;
         θON = θON + 30°;
         θOFF = θOFF + 30°;
       }
    }
   else if ((iL^ref *ω < 0) and (ω > 0))
    {
      θON = θON + 30°;
      θOFF = θOFF + 30°;
    }
   else if ((iL^ref *ω > 0) and (ω < 0))
    {
      θON ↔ θOFF;
      θON = θON + 30°;
      θOFF = θOFF + 30°;
    }
   else if ((iL^ref *ω < 0) and (ω < 0))
    {
      θON ↔ θOFF;
    }
```
(a)

```
  if   (((θ ≥ θON) and (θ ≤ θOFF)) or
       ((θ ≤ θON) and (θ ≥ θOFF)))
   {
     if (iL^ref *ω > 0)
      {
        if ((iL^ref - iL) ≥ Δi)
          STATE 1;
        else if ((iL^ref - iL) ≤ -Δi)
          STATE 2;
      }
     else (iL^ref *ω < 0)
        if ((iL^ref - iL) ≥ Δi)
          STATE 1;
        else if ((iL^ref - iL) ≤ -Δi)
          STATE 3;
   }
  else if   ((((θ > θON) and (θ > θOFF)) or
            ((θ < θOFF) and (θ < θON))) and (iL > 0))
   {
     STATE 3;
   }
  else
   {
     STATE 2;
   }
 }
else
```
(b)

Fig. 6. Control logic of the SRM drive: a) mode of operation decisions; b) PWM current control.

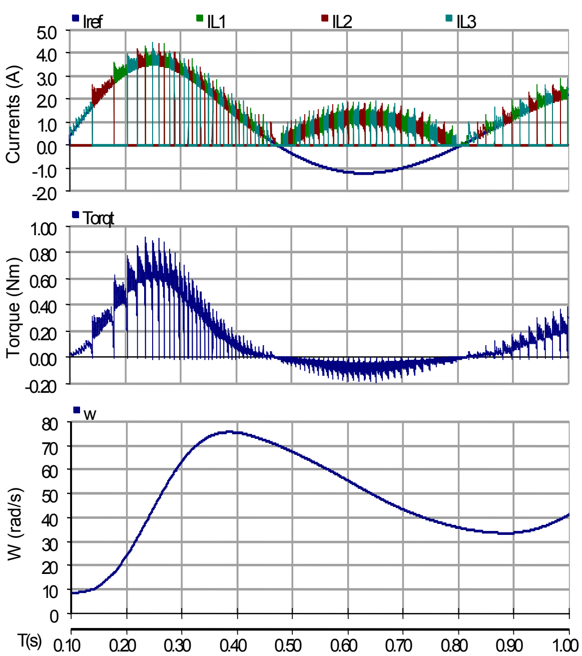


Fig. 7. Simulated speed control of a 6/4 SRM.

## V. CONCLUSION

This paper has presented a dynamic model of a flywheel based energy storage system which can take non-linearities into account. The system uses a switched reluctance machine. The machine and control models were described in detail. Some simulations were carried out, demonstrating both the correct operation of the SRM and the flywheel when connected to a generic grid. The model was confronted with experimental results for the most possible detailed case, which occurs when the system is operating in the single pulse mode. The comparison between the experimental and simulated case proves the successful modeling.

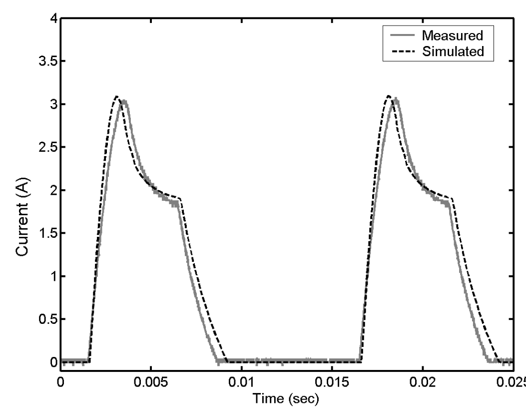


Fig. 8. Current in one stator phase in the single pulse mode: Steady State measurements and simulated results

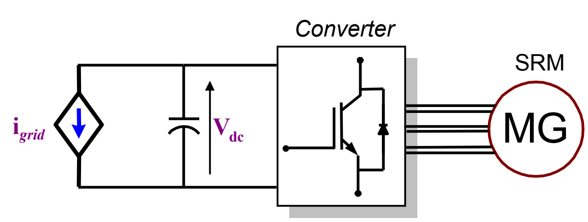


Fig 9. Flywheel energy storage system simplified circuit

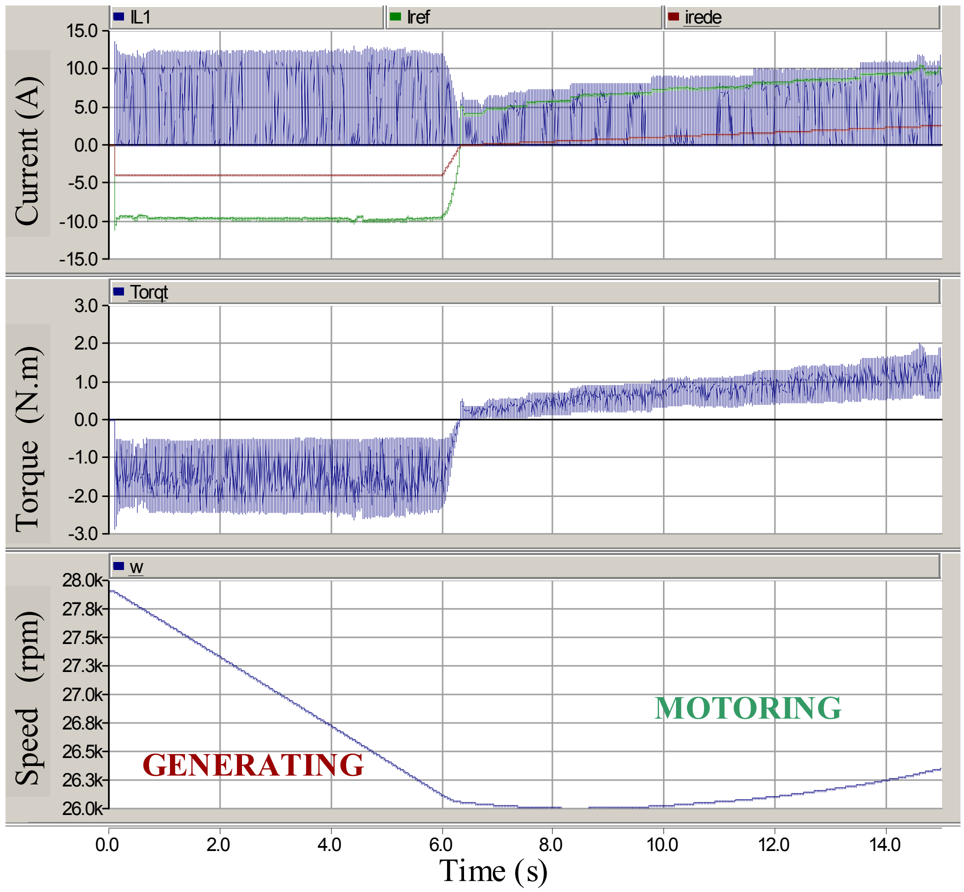


Fig 10. The simulated performance of the control loop when energy is injected or drawn from the link.

ACKNOWLEDGEMENT

This work was partially supported by Light, CNPq, FUJB and CAPES/GRISES.

REFERENCES

[1] G. Tanneau, D. Boudou, "Custom Power Interface", Proceedings of CIRED2001, pp. 2.48, June 2001.
[2] R. Hebner, J. Beno, A. Walls, "Flywheel Batteries Come Around Again", IEEE Spectrum, pp. 46-51, April 2002.
[3] K. Srinivas, R.Arumugam, "Dynamic Characterization of SRM by Computer-Aided Design and Electromagnetic Transient Simulation", IEEE Trans. on Magnetics, vol.39, pp. 1806-1812, May 2003.
[4] T. Miller, "Switched Reluctance Motors and Their Control", ISBN 0-19-859387-2, Magna Physics Publishing and Clarendon Press - Oxford, 1993.
[5] D. Torrey, "Switched reluctance generators and their control", IEEE Transactions on Industrial Electronics, Vol. 49, pp. 3-14, Feb. 2002.
[6] O. Ichinokura, T. Kikuchi, K. Nakamura, T. Watanabe, H-J.Guo, "Dynamic simulation model of switched reluctance generator", IEEE Transactions on Magnetics, Vol. 39, pp. 3253-3255, Sept. 2003.
[7] D. Torrey, J. Lang, "Modelling a nonlinear variable-reluctance motor drive", IEE Proc. - Electric Power Applications, Vol. 137, pp. 314-326, Sept. 1990.
[8] O. Ichinokura, T. Onda, T. Kimura, T. Watanabe, T. Yanada, H-J.Guo, "Analysis of dynamic characteristics of switched reluctance motor based on SPICE", IEEE Transactions on Magnetics, Vol. 34, pp. 2147-2149, July 1998.
[9] V. Vujicic, S.N. Vukosavic, "A simple nonlinear model of the switched reluctance motor", IEEE Trans. on Energy Conversion, vol. 15, pp. 395-400, Dec. 2000.
[10] P. Branco, F. Soares, "Simulation of a 6/4 switched reluctance motor based on Matlab/Simulink environment", IEEE Transactions on Aerospace and Electronic Systems, Vol. 37, pp. 989-1009, July 2001.